



**HAL**  
open science

## Thermo-mechanical stresses in cast steel dies during glass pressing process

Gilles Dusserre, Fabrice Schmidt, Gilles Dour, Gérard Bernhart

► **To cite this version:**

Gilles Dusserre, Fabrice Schmidt, Gilles Dour, Gérard Bernhart. Thermo-mechanical stresses in cast steel dies during glass pressing process. AMPT'2005 -8th International Conference on Advances in Materials and Processing Technologies, May 2005, Gliwice-Wisla, Poland. 4 p. hal-01788416

**HAL Id: hal-01788416**

**<https://hal.science/hal-01788416>**

Submitted on 5 Mar 2019

**HAL** is a multi-disciplinary open access archive for the deposit and dissemination of scientific research documents, whether they are published or not. The documents may come from teaching and research institutions in France or abroad, or from public or private research centers.

L'archive ouverte pluridisciplinaire **HAL**, est destinée au dépôt et à la diffusion de documents scientifiques de niveau recherche, publiés ou non, émanant des établissements d'enseignement et de recherche français ou étrangers, des laboratoires publics ou privés.

# Thermo-mechanical stresses in cast steels dies during glass pressing process

G. Dusserre<sup>a</sup>, F. Schmidt<sup>a</sup>, G. Dour<sup>a</sup>, G. Bernhart<sup>a</sup>

<sup>a</sup> CROMeP, Ecole des Mines d'Albi-Carmaux, Route de Teillet, 81013 Albi Cedex 09, France

## Abstract

Cast steels dies used in glass pressing process present dispersal in their lifetime in spite of apparently similar pressing parameters. These dispersal does not seem to be due to casting defects because every mold presents such defects. In order to know if undetectable variations of any process parameter could produce such lifetime dispersal, a finite element simulation of glass pressing process is here proposed. In this paper, glass is supposed to be a Newtonian fluid, cast steel is considered as a thermo-elastic material, thermal transfer between glass and mold depend only on time and radiative heat transfer in glass is taken into account by Rosseland diffusion approximation. The validation of the results of this simulation is made by comparison of the calculated pressing force to the experimental one. Although the experimental data introduced in the simulation does not have been measured in the industrial process, the order of magnitude of the calculated pressing force is similar to the real one.

*Keywords:* Glass Pressing Process; Numerical Simulation; Thermo-mechanical Stresses; Rosseland Diffusion Approximation;

## 1. Introduction

Glass pressing is a forming process that realizes hollow parts in only one stage (Fig. 1). The glass is heated up to 1500°C in a furnace and then cooled near 1250°C in the feeder. The gob is formed and fall into the lower mould preheated at 450°C. The gob shape then between the lower and the upper mould, activated by an hydraulic press. These tools are made of cast martensitic stainless steel GX30Cr13 (norm NF EN 10027-1 and Table 1). This process involves high temperature, high strain rate, thermal and mechanical stresses, fatigue phenomena, oxidation and complex moulds shape which lead to appearance of cracks on the lower mould surface. These cracks are initiated on casting defects (shrinkage).

The lifetime of the mould is determined by the dimensions of these cracks : no trace must be visible on the finished part. It as been observed that the so defined lifetime could be very different (factor 2) between two moulds of the same batch, whereas the process parameters don't seem to have vary.

This paper presents a finite element simulation of the glass pressing process to calculate the thermo-mechanical stresses in the dies. This simulation could allow to identify process parameters which small variation could involve significant stresses variation. The software FORGE2<sup>®</sup> was used because he authorizes a precise description of the cinematic of the process and possess an automatic remeshing module. To minimize time calculation, axisymmetric calculation will be realized. The parameters that influence the most the stresses in the mould are : the rheological behavior of glass, the mechanical behavior of the

steel, the radiative heat flux in the glass, the heat flux density at gob/mould interface and the friction between glass and mould.

## 2. Input data of the simulation

### 2.1. Rheological behavior of glass

The glass studied is Pyrex<sup>®</sup> (Table 2). It is a borosilicate glass with a low expansion coefficient in order to resist up to 300°C.

Rheological behavior of glasses is very temperature dependant [1]. At low temperature, glasses behave like a brittle elastic solid; around the glass transition temperature, it behave like a thermo-rheological simple visco-elastic material [2-4]; and at high temperature it behaves like a viscous fluid [5-7].

Non-Newtonian behavior could be observed [8] : the viscosity of the glass melt decrease with the increase of strain rate. In this paper, the glass is supposed to be a Newtonian fluid (Eq.1), that means that the viscosity will be assume to vary only with the temperature as described by the Tammann-Vogel-Fulcher (TVF) equation (Eq. 2 and Fig. 2) [9].

$$\underline{s} = 2\eta(T)\dot{\underline{\epsilon}} \quad (1)$$

$$\log \eta = A + \frac{B}{T - T_0} \quad (2)$$

Where  $\underline{s}$  is the deviatoric part of the Cauchy stress tensor,  $\eta$  is the glass viscosity,  $\dot{\underline{\epsilon}}$  is the strain rate tensor, T is the temperature and A, B, T<sub>0</sub> are constants.

\* Corresponding author.

E-mail address : gilles.dusserre@enstimac.fr

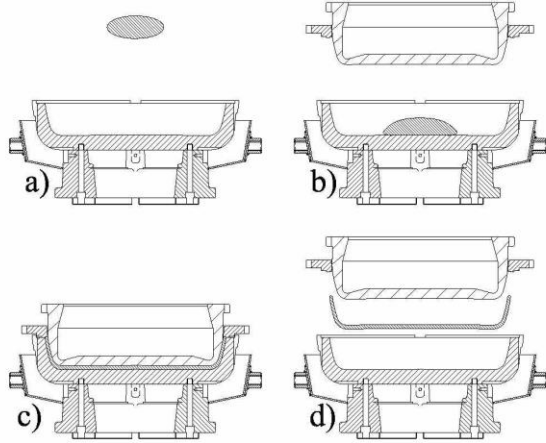


Fig.1. Main stages of the glass pressing process : a) delivery, b) pressing, c) pressure maintenance, d) takeout

Table 1.

Chemical composition (wt.%) of GX30Cr13 steel

C	Cr	Si	Mn	Ni
0.3	13	0.6	0.9	<0.5

Table 2.

Chemical composition (wt.%) of Pyrex® glass

SiO <sub>2</sub>	B <sub>2</sub> O <sub>3</sub>	Na <sub>2</sub> O	Al <sub>2</sub> O <sub>3</sub>	K <sub>2</sub> O	CaO	MgO	TiO <sub>2</sub>	FeO
82.57	10.81	5.13	1.23	0.13	0.05	0.05	0.02	0.01

## 2.2. Mechanical behavior of GX30Cr13 steel

It will be assumed that the steel of the mould behave as a thermo-elastic solid (Fig. 3). Young's modulus will be introduced in the software FORGE2® as a function of temperature (Fig. 3) and Poisson's ratio will be equal to 0.3.

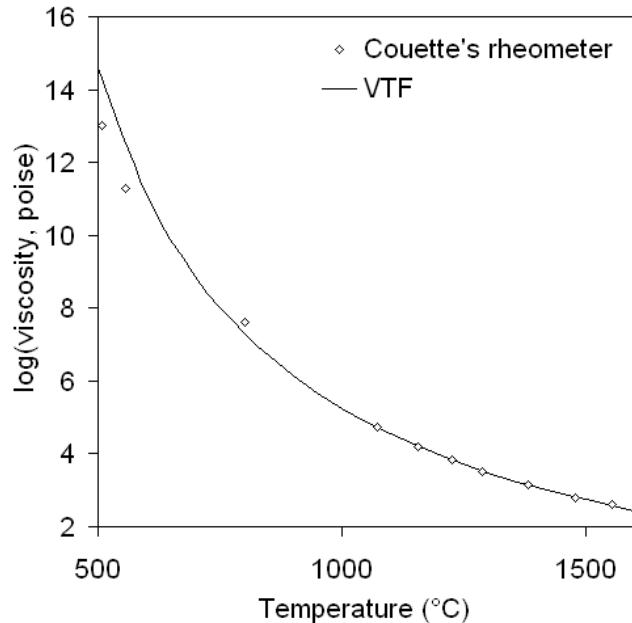


Fig. 2. Temperature dependency of the viscosity of Pyrex® : experimental points and VTF equation

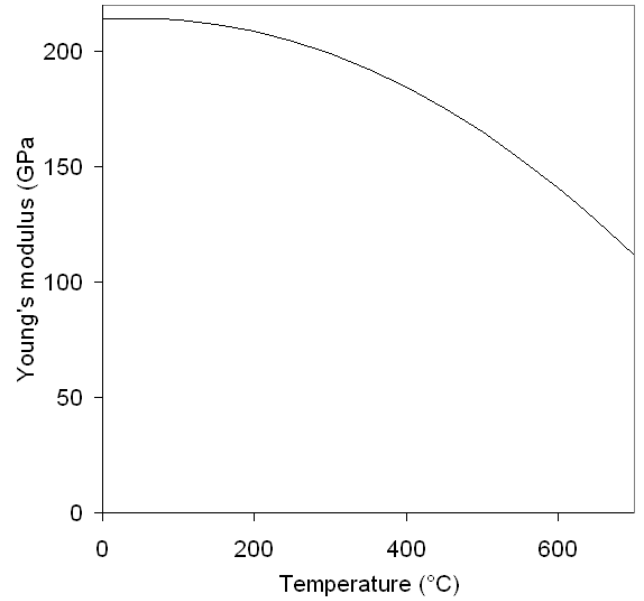


Fig. 3. Young's modulus of GX30Cr13 steel as a function of temperature

## 2.3. Conductive and radiative heat transfer in glass

The high temperature dependency of the glass rheological behavior involves the necessity of a precise thermal computation. Glass being a semi-transparent media, heat transfer occur not only by conduction but also by radiation. Thermal conductivity ( $W.m^{-1}.K^{-1}$ ) of glass is supposed to vary with temperature (K) as described by Loulou et al. (cf. [10] and Eq. 3).

$$k_{cond} = 0.7222 + 0.001583 (T - 273) \quad (3)$$

Radiative heat transfer is a very complex phenomena because heat flux in one point of the gob is influenced by every other point of the glass part. The easiest way to take the radiative heat transfer into account is to use a diffusion approximation : a radiative conductivity is defined as a function of the temperature, radiative and conductive heat fluxes are then calculated by Fourier's law. An expression of this radiative conductivity  $k_{rad}$  was proposed by Rosseland [11] (Eq. 4 and Fig. 4).  $n$  is the refractive index of the semi-transparent media,  $\sigma$  is the Stefan-Boltzmann constant,  $T$  is the temperature in K and  $\bar{\kappa}_{Ross}$  is the Rosseland mean extinction coefficient defined by Eq. 5.  $\nu$  is the frequency of the radiation,  $\kappa(\nu)$  is extinction coefficient and  $B(\nu, T)$  is the blackbody intensity as described by the Planck's function.

$$k_{rad}(T) = \frac{16n^2\sigma}{3\bar{\kappa}_{Ross}(T)} T^3 \quad (4)$$

$$\frac{1}{\bar{\kappa}_{Ross}(T)} = \frac{\int_0^\infty \frac{1}{\kappa(\nu)} \frac{\partial B(\nu, T)}{\partial T} d\nu}{\int_0^\infty \frac{\partial B(\nu, T)}{\partial T} d\nu} \quad (5)$$

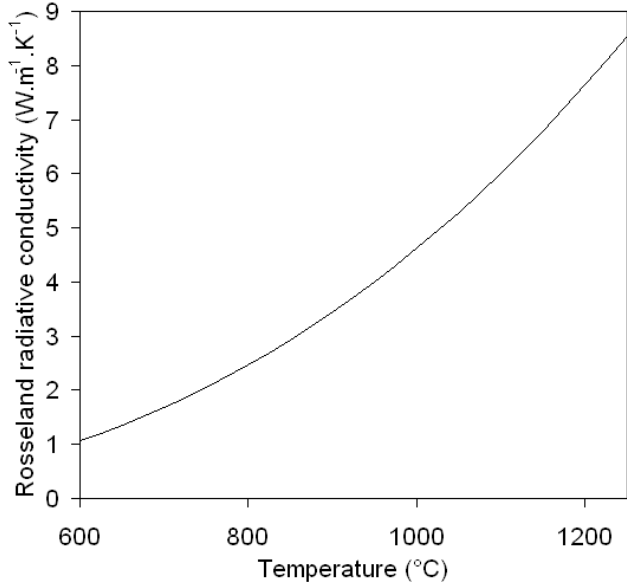


Fig. 4. Rosseland radiative conductivity of Pyrex® as a function of temperature

This method is very easy to compute, but the assumption is made, that the glass is optically thick. This means, that the most of the radiation is absorbed in the neighborhood of the particle that emitted it. This assumption is not valid for a glass domain with small dimensions, as in the present case.

Analytical solution of the Radiative Transfer Equation is available in the one-dimensional case, but it requires to know the optical properties of the glass and the surface of the mould, and strong assumptions are made on the geometry of the problem [10, 12].

Numerical methods could be used as Discrete Ordinate Method, Improved Diffusion Approximation, Ray Tracing, Monte Carlo [10, 13], but they require long calculation time.

In a first time, radiative heat transfer will be neglected because analytical and numerical methods are not easy to introduce in FORGE2®.

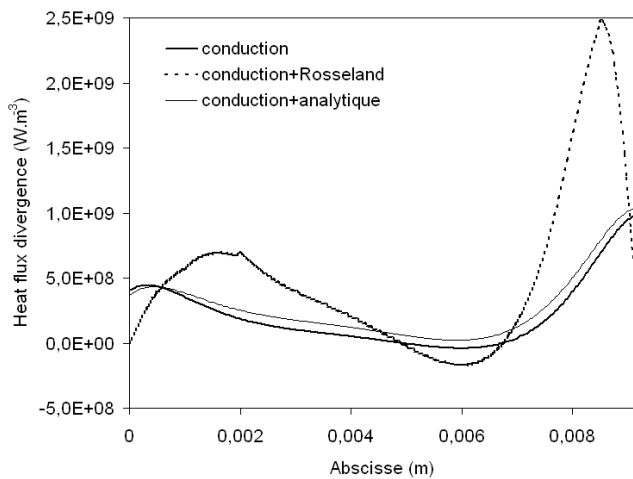


Fig. 5. Comparison of profile of heat fluxes divergence in the one-dimensional case for Rosseland diffusion approximation, analytical method and without radiation

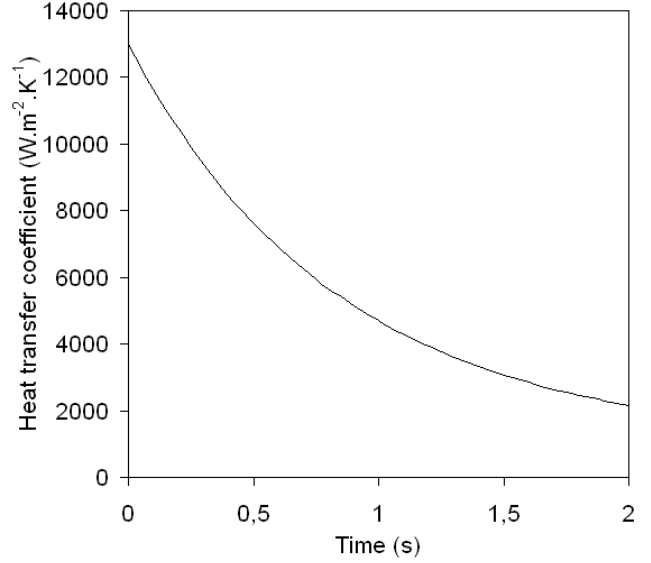


Fig. 6. Heat transfer coefficient at glass/mould interface as a function of time

Fig. 5 presents the profile of heat flux divergence in the glass supposed to be an infinite plate for a computed temperature profile calculated with Rosseland diffusion approximation, analytical method ([10, 13]) and without radiation effects. It could be observed that in this case, the Rosseland method over-evaluates heat fluxes divergence compared to analytical method. In a first time, it will be assumed that radiative heat transfer could be neglected compared to conductive heat transfer.

#### 2.4. Heat flux density at gob/mould interface

The second function of a mould being to cool the glass, the thermal computation requires to know the heat flux density exchanged between the gob and the mould. Experiments have been made [10, 14, 15] to measure heat flux at the glass/mould interface as a function of time. Semi-empirical models have been developed by decoupling radiative and convective part of the flux. For example, Pchelyakov [10, 16, 17] proposed a heat transfer coefficient equal to the conductivity divided by the thickness of a gap between gob and mould. The experimental results of Moreau et al. [15] (Fig. 6) will be used in this paper.

#### 2.5. Friction between glass and mould

Friction between glass and steel is largely influenced by the temperature of the glass at the interface. Studies have been led on friction between glass and steel in the condition of delivery gobs into moulds [19]. Li et al. [20] investigated the influence of temperature and strain rate on the friction at the interface during compression test of titanium rings lubricated with glass. Below 950°C, strain rate does not seem to play a significant role on friction behavior. These results will be used in this paper: it is supposed that glass temperature at the interface is 750°C, and that friction behavior follows the Tresca model with a friction factor  $\bar{m}$  equal to 0.28 (Eq. 6). In Eq. 6,  $\tau$  is the shear stress and  $\Delta\vec{V}$  is the difference between the velocity of the glass and the velocity of the mould.

$$\tau = -\bar{m} \eta(T) \frac{\Delta\vec{V}}{\|\Delta\vec{V}\|} \quad (6)$$

## 2.6. Heat capacity of Pyrex®

Heat capacity of Pyrex® has been introduced in FORGE2® as a function of the temperature has described by Richet et al. [21].

## 3. Simulation of the gob loading in the mould

### 3.1. Initial conditions

The first stage of the glass pressing process that has been chosen to simulate is loading of the gob in the mould. The initial gob shape, gob mesh and temperature distribution are presented in Fig. 7. The initial temperature distribution corresponds to a 0.5 s cooling in contact with a loading chute at 100°C on the lower side (heat transfer coefficient 2000 W.m<sup>-2</sup>.K<sup>-1</sup>) and convection with air on the other ones (heat transfer coefficient 150 W.m<sup>-2</sup>.K<sup>-1</sup> [22]). The gob has been placed at a distance of 50 mm from the mould and falls freely. The initial shape, mesh and temperature distribution of the mould are shown in Fig. 8. The initial temperature distribution is the result of a 30 s cooling by convection in free air (heat transfer coefficient 10 W.m<sup>-2</sup>.K<sup>-1</sup>) corresponding to the time between loading the mould on the press and first pressing.

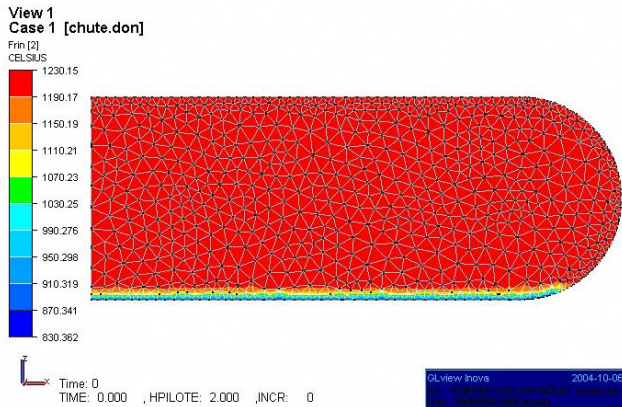


Fig. 7. Initial condition of the gob for the loading stage

### 3.2. Boundary conditions

Thermal exchanges considered are convection with air during loading of the gob, convection between the mould and air, and thermal exchanges between mould and glass. The heat transfer coefficient between gob and air is equal to 150 W.m<sup>-2</sup>.K<sup>-1</sup>, as it can be interpolated at 1100°C from the results of the inverse method proposed by Locheignies and Marechal [22]. Convection coefficient between air and steel as been set to 10 W.m<sup>-2</sup>.K<sup>-1</sup> (the default value proposed by FORGE2®). Heat transfer coefficient as been defined as a function of time (section 2.4. and Fig. 6).

Friction between glass and steel is defined in section 2.5.

### 3.3. Results

The total time of the simulation is 2 s. The final configuration of this simulation will be defined as initial configuration of the pressing stage (Fig. 9). Fig. 10 present the variation of the Mises equivalent stress at the surface of the mould on the axis during gob loading simulation and Fig.11 shows the temperature at the same point. The maximum Mises equivalent stress reaches 430 MPa at 515°C (the maximum temperature reached is 520°C). Mechanical behavior of GX30Cr13 cast steel should be studied in details, but it could be supposed, that this stress could at least provoke local plastic deformation in the shrinkage zones where stress concentration may occur, and lead to cracks appearance.



Fig. 8. Initial condition of the mould for the loading stage



Fig. 9. Initial configuration and temperature distribution for the pressing stage

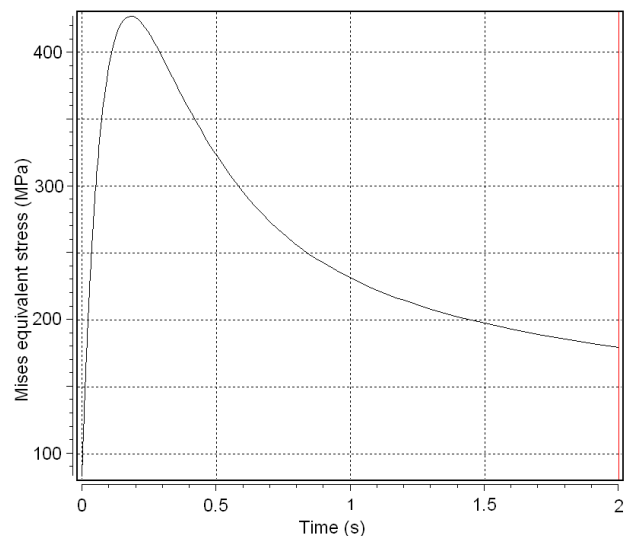


Fig. 10. Evolution of Mises equivalent stress at the surface of the mould with time during gob loading.

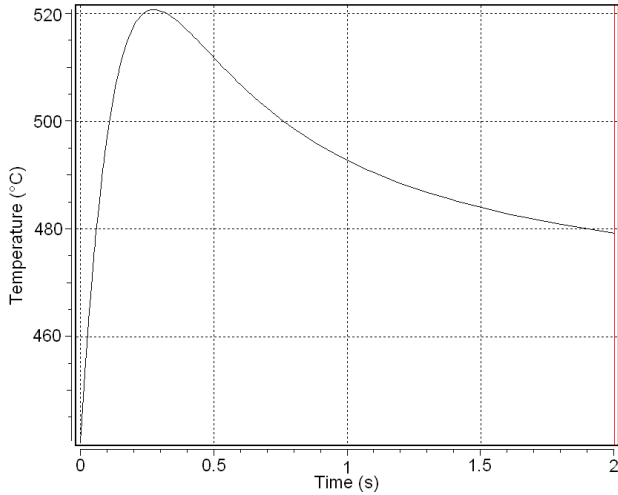


Fig. 11. Evolution of temperature at the surface of the mould with time during gob loading

#### 4. Simulation of the pressing

##### 4.1. Initial conditions

The second stage of the process that has been simulated is pressing. The initial configuration corresponds to the final one of the gob loading stage. Fig. 9 shows the initial temperature distribution in the gob and in the lower mould. Initial temperature of the upper mould has been set to a uniform value (250°C).

##### 4.2. Boundary conditions

The boundary conditions for this simulation are the same as for gob loading, except the heat transfer coefficient between gob and moulds that has been set to a constant value (2000 W.m<sup>-2</sup>.K<sup>-1</sup>). It has been supposed that effect of pressure on heat transfer coefficient is negligible and that his value is the final one of the gob loading stage (Fig. 6). The inner surface of the upper mould is cooled by a 20°C water flow.

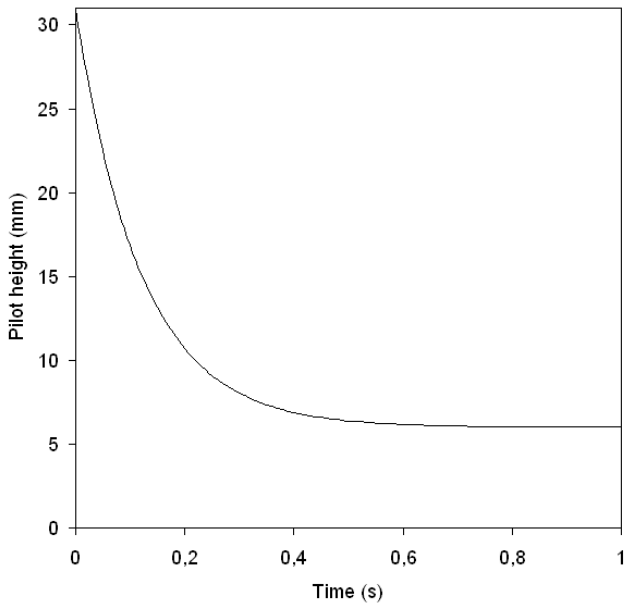


Fig. 12. Piloting height as a function of time.

##### 4.3. Press piloting

The lower mould is fixed and the upper one is piloted with a height-time curve (Fig. 12). This curve has been interpolated from initial height, final height and initial velocity by an exponential function (Eq. 7).

$$h(t) = 6 + 25 * e^{-8.335*t} \quad (7)$$

Where h is the piloted height (mm) and t is time (s).

##### 4.4. Results

Final temperature distribution in gob and moulds is shown Fig. 13. Mises equivalent stress at the surface of the mould on the axis has been plotted as a function of time on Fig. 14 and temperature at the same point on Fig. 15. The maximum Mises equivalent stress is 850 MPa at 489°C. As it could be seen on Fig. 16, there is an other zone where stresses are important (in the edge of the plane surface of the mould). In this point, maximum Mises equivalent stress is not so important as on the axis but a high stress level exists. The evolution of the stress at this point during pressing is plotted Fig. 16. It could be concluded that as for loading stage, plastic deformation could occur during pressing around the shrinkages.



Fig. 13. Temperature distribution in gob and moulds at the end of pressing

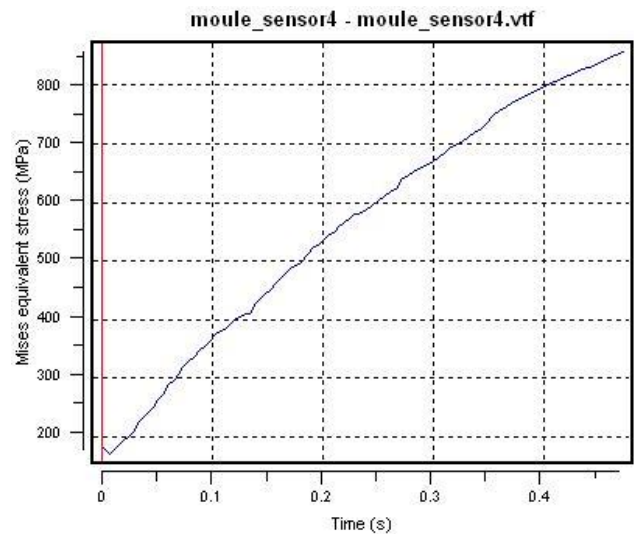


Fig. 14.a. Evolution of Mises equivalent stress at the surface of the mould on the axis with time during pressing

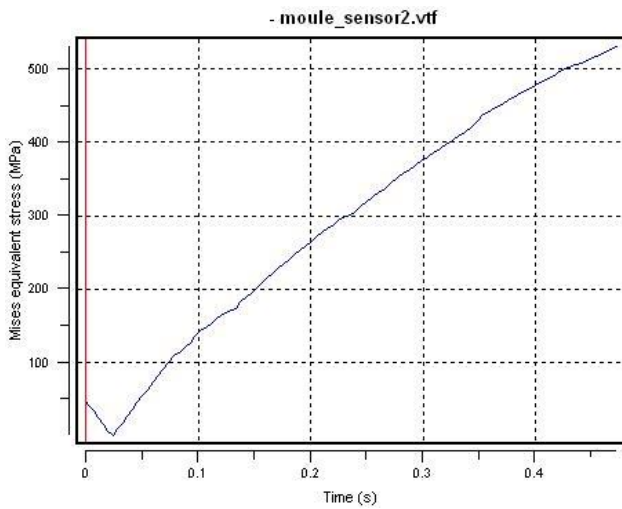


Fig. 14.b. Evolution of Mises equivalent stress at the surface of the mould in the edge of the plane surface with time during pressing

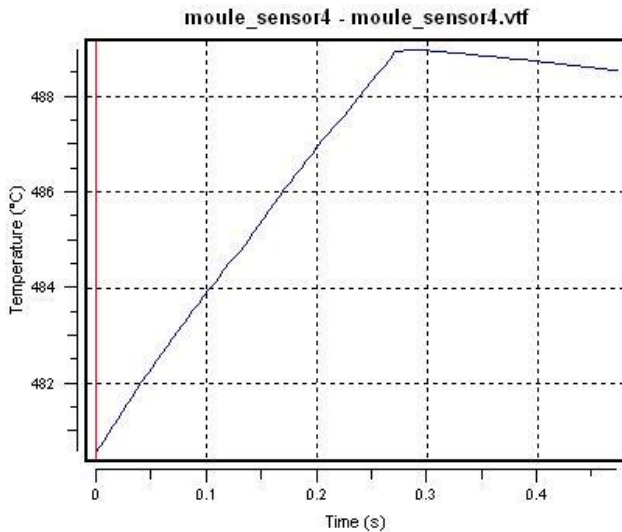


Fig. 15. Evolution of temperature at the surface of the mould with time during pressing

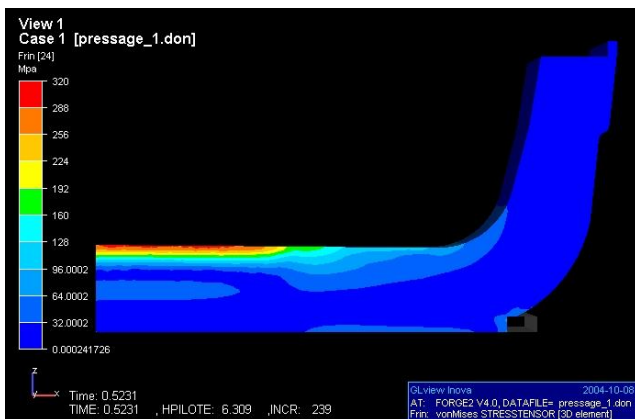


Fig. 16. Mises equivalent stress distribution in lower mould during pressing

## 5. Conclusion

To validate this numerical results with experimental data, computed pressing force has been compared with the real one (the industrial process use a 5.4 tons hydraulic press). The calculated force has been plotted on Fig. 17. Although the models that have been introduced in the software are not very precise (Rosseland approximation) or corresponds to conditions that are not exactly similar to the ones of our case, the order of magnitude of the computed pressing force is realist but largely over evaluated. The difference between the calculated and the real pressing force could largely be explained by the piloting of the press in the pressing simulation which does not corresponds to measurement (the velocity is not described on a realist way).

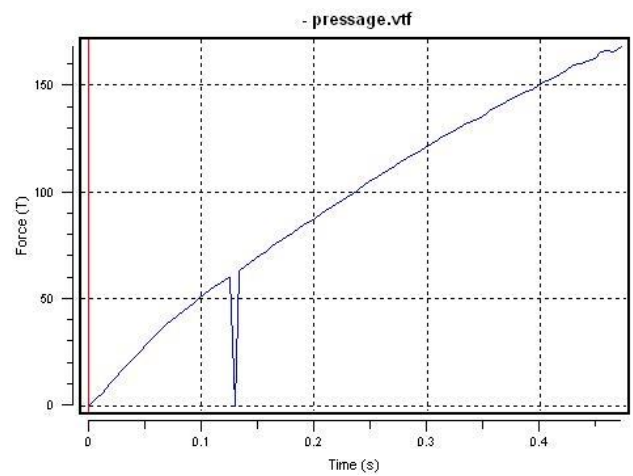


Fig. 17. Computed pressing force as a function of time

Even if the stresses in the mould are over-evaluated (as the pressing force), it could has been observed that cracks appearance could occur at two locations in the mould : at the center or at the edge of the plane surface. The first zone is solicited both thermally and mechanically, whereas the second one is almost solicited mechanically. It could has been observed that industrials moulds present cracks in one or the other of these two zones depending on the shape of the mould : few proof and axisymetric moulds are damaged at the center whereas proof and elliptic moulds are damaged at the edge of the plane surface.

This simulation could be improved by taking experimental data into account (glass rheology, mechanical behavior of GX30Cr13 steel, radiative effects, heat flux density at the gob/mould interface, piloting of the press...) and then be used to study the influence of process parameters on moulds lifetime (initial glass and mould temperature, pressing velocity...). Others mould materials could also be tried.

## Acknowledgements

The present investigation has been carried out with the financial support of Aubert et Duval Alliages, Newell S.A and Saint-Gobain SEVA.

## References

- [1] J. Zarzycki, *Glasses and the vitreous state*, Cambridge University Press, 1991.
- [2] P. Wiertel, D. Locheignies and J. Oudin, Optimization techniques for flat glass tempering, *Proceedings of the Colloquium on Modelling of Glass Forming Processes*, Valenciennes, France, 1998, 219-227.
- [3] H. Hessenkemper and R. Brückner, Elastic constants of glass melts above the glass transition temperature from ultrasonic and axial compression measurements, *Glastechnische Berichte*, 64 (1991) No. 2 29-38.
- [4] M. Van Iseghem, L. Fourment, J.F. Agassant, Residual stress simulation in a glass/metal contact, *Proceedings of the Colloquium on Modelling of Glass Forming Processes*, Valenciennes, France, 1998, 253-261.
- [5] D. Locheignies, C. Marion, E. Carpentier and J. Oudin, Finite element contributions to glass manufacturing control and optimization. Part 2. Blowing, pressing and centrifuging of hollow items, *Glass Technology* 37 No. 5 (1996) 169-174.
- [6] A. Milutinović-Nikolić, R. Jančić and R. Aleksić, Mathematical modelling and simulation of drawing thin glass sheet from a rectangular perform, *Glass Technology* 39 No. 5 (1998) 166-172.
- [7] M. Hyre and A. Leven Harrison, Effect of feeder design and operation on gob shape, *Verre* 9 No.2 (2003) 20-23.
- [8] Y. Yue and R. Brückner, On the different descriptions of the non-Newtonian viscosity (shear-thinning effect) of glass melts with respect to heat dissipation, *Glastechnische Berichte*, 69 (1996) No. 6 179-185.
- [9] A. Sipp, D.R. Neuville and P. Richet, Viscosity, configurational entropy and relaxation kinetics of borosilicate melts, *Journal of Non-Crystalline Solids* 211 (1997) 281-293.
- [10] T. Loulou, R. Abou-Khachfe and J.P. Bardon, Estimation de la résistance thermique de contact durant la solidification du verre, *International Journal of Thermal Sciences* 38 (1999) 984-998.
- [11] F.T. Lentes and N. Siedow, Three-dimensional radiative heat transfer in glass cooling processes, *Glass Science and Technology* 72, No. 6 (1999) 188-196.
- [12] S. André, V. Manias, B. Rémy, M. Lazard and D. Maillet, A reduced analytical model for solving heat transfer in glasses, *Proceedings of the Colloquium on Modelling of Glass Forming Processes*, Valenciennes, France, 1998, 47-54.
- [13] B.J. van der Linden, R.M.M. Matheij and M. Slobt, Radiative heat transfer in hot glass melts, *Proceedings of the Colloquium on Modelling of Glass Forming Processes*, Valenciennes, France, 1998, 95-108.
- [14] D. Locheignies, C. Noiret, C. Thibaud and J. Oudin, Computation procedure for the temperature in hot glass. Application to the finite element simulation of hollow glass forming, *Glass Science and Technology* 69, No. 8 (1996) 253-264.
- [15] P. Moreau, S. Grégoire, D. Locheignies, Experimental methodology for the determination of the heat transfer coefficient at the glass/mould interface, *Verre* 9 No. 2 (2003) 24-27.
- [16] R. Viskanta, J. Lim, Analysis of heat transfer during glass forming, *Glass Science and Technology* 74, No. 11/12 (2001) 341-352.
- [17] K. Storck, D. Loyd, Heat transfer modeling of the parison forming in glass manufacturing, *Glass Technology* 39 No. 6 (1998) 210-216.
- [18] E. Brauns, J. Patyn, Finite element calculation of thermomechanical stresses in candidate ceramic components for press and blow moulds, *Glass Technology* 40 No. 2 (1999) 58-64.
- [19] M. Falipou, F. Sicloroff and C. Donnet, New method for measuring the friction between hot viscous glass and metals, *Glass Science and Technology* 72, No. 3 (1999) 59-66.
- [20] L.X. Li, D.S. Peng, J.A. Liu, Z.Q. Liu, Y. Jiang, An experimental study of the lubrication behavior of A5 glass lubricant by means of the ring compression test, *Journal of Materials Processing Technology* 102 (2000) 138-142
- [21] P. Richet, M. Ali Bouhifd, P. Courtial, C.Téqui, Configurational heat capacity and entropy of borosilicate melts, *Journal of Non-Crystalline Solids* 211 (1997) 271-280.
- [22] D. Locheignies and C. Marechal, Inverse determination of glass viscosity and heat transfer coefficient by industrial testing, *Glass Science and Technology* 75, No. 6 (2002) 304-312.